

# Exclusive electroproduction of $J/\psi$ mesons

H.G. Dosch

*Institut für Theoretische Physik, Universität Heidelberg  
Philosophenweg 16, D-6900 Heidelberg, Germany*

E. Ferreira

*Instituto de Física, Universidade Federal do Rio de Janeiro  
C.P. 68528, Rio de Janeiro 21945-970, RJ, Brazil*

(Dated: February 1, 2008)

## Abstract

A nonperturbative calculation of elastic electroproduction of the  $J/\psi$  meson is presented and compared to the experimental data. Our model describes well the observed dependences of the cross sections on the photon virtuality  $Q^2$  and on the energy, and the measured ratio  $R = \sigma_L/\sigma_T$  of longitudinal to transverse cross sections.

PACS numbers: 12.38.Lg, 13.60.Le

Keywords: electroproduction, DIS, photoproduction, vector mesons, stochastic vacuum model,  $J/\psi$

## I. INTRODUCTION

In a previous paper [1] we have investigated photoproduction of heavy mesons off protons, finding good agreement between experiment and our calculations based on a nonperturbative approach to high energy scattering [2, 3], where no free parameters had to be introduced. In this letter we present the results for electroproduction of  $J/\psi$  mesons, and compare our results with the published HERA data.

In the perturbative approach to electroproduction of heavy mesons the coupling of the exchanged gluons to the heavy vector mesons is treated perturbatively, while for the coupling of the gluons to the proton an external nonperturbative quantity, the gluon density in the proton, has to be introduced. In our approach to photo- and electroproduction of heavy mesons, the small system, the  $\gamma^* - J/\psi$  transition overlap, and the large system, the proton, are treated on the same footing and the treatment of high energy scattering is based on functional integrals [2, 4], which are evaluated in a nonperturbative approach to QCD, the stochastic vacuum model [5, 6]. It has been shown [7] that this nonperturbative approach also implies factorisation in the sense that genuine nonperturbative effects in the small system can be absorbed into the large system, that is the proton in the present case. Although our nonperturbative approach is more model dependent than the perturbative calculation, it offers the advantage that purely hadronic reactions are described with the same set of parameters as photo and electroproduction processes. Therefore in our calculations of heavy vector meson production no new parameters are introduced and the Regge model can be applied directly. Furthermore the influence of confinement effects in the small system can be studied. The WKB framework underlying our model also allows to calculate the dependence of the production processes on (moderate) momentum transfer, which is not directly possible in the perturbative approach.

## II. BASIC FORMULÆ AND GENERAL RESULTS

For convenience we present here some basic formulae developed in our previous work on photoproduction [1], where motivation and details can be found.

The electroproduction amplitude of vector mesons is written

$$T_{\gamma^* p \rightarrow V p, \lambda}(t) = \int d^2 R_1 dz_1 \psi_{V\lambda}(z_1, R_1)^* \psi_{\gamma^*\lambda}(z_1, R_1, Q^2) J(\vec{q}, z_1, \vec{R}_1) , \quad (2.1)$$

with

$$J(\vec{q}, z_1, \vec{R}_1) = \int d^2 R_2 d^2 b e^{-i\vec{q}\cdot\vec{b}} |\psi_p(R_2)|^2 S(b, z_1, \vec{R}_1, z_2 = 1/2, \vec{R}_2) . \quad (2.2)$$

Here  $S(b, z_1, \vec{R}_1, 1/2, \vec{R}_2)$  is the scattering amplitude of two dipoles with separation vectors  $\vec{R}_1, \vec{R}_2$ , colliding with impact parameter vector  $\vec{b}$ ;  $\vec{q}$  is the momentum transfer of the reaction

$$t = -\vec{q}^2 - m_p^2(Q^2 + M_V^2)/s^2 + O(s^{-3}) \approx -\vec{q}^2 . \quad (2.3)$$

The differential cross section is given by

$$\frac{d\sigma}{d|t|} = \frac{1}{16\pi s^2} |T|^2 . \quad (2.4)$$

The wave functions of the photon and vector meson have been discussed extensively in ([1]), where it has been shown that the results obtained with different forms of the meson

wave function are very similar. We use here only the Bauer-Stech-Wirbel (BSW) [8] type of wave function, which is of the general form

$$\psi_{V\lambda}(z_1, R_1) = f(z_1) \exp[-\omega^2 R_1^2/2] \times \text{helicity dependent factors} , \quad (2.5)$$

where  $f(z_1)$  contains the normalisation constant and the  $z_1$ -dependence of the meson wave function, with the form

$$f(z) = \frac{N}{\sqrt{4\pi}} \sqrt{z(1-z)} \exp \left[ -\frac{M_V^2}{2\omega^2} \left( z - \frac{1}{2} \right)^2 \right] . \quad (2.6)$$

The size of the vector meson is determined by  $\omega$ , which is fixed by the leptonic decay width of the meson.

After summation over helicity indices, the overlaps of the photon and vector meson wave functions are given by

$$\begin{aligned} \rho_{\gamma^*, V, \pm 1}(z_1, R_1, Q^2) &= \psi_{V, \pm 1}(z_1, R_1)^* \psi_{\gamma^*, \pm 1}(z_1, R_1, Q^2) = \\ &\hat{e}_f \frac{\sqrt{6\alpha}}{2\pi} f(z_1) \exp[-\omega^2 R_1^2/2] \\ &\times \left( \epsilon \omega^2 R_1 [z_1^2 + (1-z_1)^2] K_1(\epsilon R_1) + m_f^2 K_0(\epsilon R_1) \right) \\ \rho_{\gamma^*, V, 0}(z_1, R_1, Q^2) &= \psi_{V, 0}(z_1, R_1)^* \psi_{\gamma^*, 0}(z_1, R_1, Q^2) = \\ &-16 \hat{e}_f \frac{\sqrt{3\alpha}}{2\pi} \omega f(z_1) \exp[-\omega^2 R_1^2/2] z_1^2 (1-z_1)^2 Q K_0(\epsilon R_1) . \end{aligned} \quad (2.7)$$

Here

$$\epsilon = \sqrt{z_1(1-z_1)Q^2 + m_f^2} ,$$

$K_0, K_1$  are the modified Bessel functions,  $\lambda = \pm 1$  and  $0$  denote transverse and longitudinal polarisations of the vector meson and the photon,  $m_f$  is the quark mass and  $\hat{e}_f$  is the quark charge in units of the elementary charge for each flavour  $f$ . All parameters are fixed from other processes (see [1]) and all observables can be calculated from (2.1).

The energy dependence in our model is motivated by the two-pomeron model of Donnachie and Landshoff [9]. For  $R_1 \leq r_c \approx 0.22$  fm the coupling through the hard pomeron induces the energy dependence  $(s/s_0)^{0.42}$ , while the coupling of large dipoles follows the soft pomeron energy dependence  $(s/s_0)^{0.0808}$ . The reference energy is  $s_0 = (20 \text{ GeV})^2$ . We therefore split the integration over  $R_1$  appearing in (2.1) into two parts, as fully described in our study of  $J/\psi$  photoproduction [1].

Before proceeding to the comparison with experimental data we wish to present some general approximate features of our model which describe the overall situation quite well and provide a background against which finer details can be studied.

If  $R_1$  is small compared to the extension of the proton and  $|t| = \vec{q}^2 < 1 \text{ GeV}^2$ , we obtain after integration over the azimuthal angle of  $\vec{R}_1$ , the simple expression for the amplitudes

$$T_{\gamma^* p \rightarrow V p}^\lambda(t) \approx (-2is) 2\pi \frac{C e^{-a|t|}}{1+b|t|} \int dR_1 dz_1 R_1^3 e^{-\eta R_1^2 |t|} \rho_{\gamma^*, V, \lambda}(z_1, R_1, Q^2) . \quad (2.8)$$

For the case of  $J/\psi$  production the numerical values for the constants in (2.8) are

$$C = 2.28, \quad a = 0.847 \text{ GeV}^{-2}, \quad b = 3.85 \text{ GeV}^{-2}, \quad \eta = 0.059 . \quad (2.9)$$

This result means that the integrated expression in (2.2) is proportional to  $R_1^2 \exp[-\eta R_1^2 |t|]$  and that the main  $t$  dependence in the amplitude is factorized out, being independent of  $Q^2$  and of  $W$ .

Since in the overlap functions with heavy vector mesons  $\eta R_1^2$  is very small, the exponential factor  $e^{-\eta R_1^2 |t|}$  can be extracted from the integral in (2.8), and represented by an external factor  $e^{-\eta R_m^2 |t|}$ , where  $R_m$  is an appropriate mean value of  $R_1$ . The numerical calculation shows that a very good representation for the  $Q^2$  dependence of this external factor is given by  $R_m^2 \approx 12/(Q^2 + M_V^2)$ .

We can then write for the scattering amplitude

$$T_{\gamma^* p \rightarrow V p}^\lambda(s, t; Q^2) \approx (-2is) \frac{C e^{-a|t|}}{1 + b|t|} \exp \left[ -12\eta |t| / (Q^2 + M_V^2) \right] \\ \times \left( T_h^\lambda(Q^2) \left( \frac{s}{s_0} \right)^{\epsilon_h} + T_s^\lambda(Q^2) \left( \frac{s}{s_0} \right)^{\epsilon_s} \right) \quad (2.10)$$

with

$$T_h^\lambda(Q^2) = 2\pi \int_0^{r_c} dR_1 dz_1 \left( \frac{R^2}{r_c^2} \right)^{\epsilon_h} R_1^3 \rho_{\gamma, V, \lambda}(Q^2, z_1, R_1), \\ T_s^\lambda(Q^2) = 2\pi \int_{r_c}^\infty dR_1 dz_1 R_1^3 \rho_{\gamma, V, \lambda}(Q^2, z_1, R_1). \quad (2.11)$$

The parameters for the energy dependence are  $s_0 = (20 \text{ GeV})^2$ ,  $\epsilon_h = 0.42$ ,  $\epsilon_s = 0.0808$ .

Eq. (2.10) allows us to express all observables through the functions  $T_h^\lambda(Q^2)$  and  $T_s^\lambda(Q^2)$  (2.11). We display these amplitudes in Fig. 1. They can be parametrized for the range  $0 \leq Q^2 \leq 100 \text{ GeV}^2$  in the forms

$$T_s^{\pm 1}(Q^2) = 0.0267 / (1 + \frac{Q^2}{15.03})^{2.71}, \\ T_h^{\pm 1}(Q^2) = 0.00488 / (1 + \frac{Q^2}{20.46})^{1.72}, \quad (2.12)$$

$$T_s^0(Q^2) = -0.00635 Q / (1 + \frac{Q^2}{18.00})^{3.23}, \\ T_h^0(Q^2) = -0.00170 Q / (1 + \frac{Q^2}{20.61})^{1.9}, \quad (2.13)$$

where  $Q^2$  is measured in  $\text{GeV}^2$ .

The overall  $|t|$  dependence determined by the form factor

$$F(|t|) = \frac{e^{-a|t|}}{1 + b|t|} \exp[-12\eta |t| / (Q^2 + M_V^2)]$$

yields a characteristic curvature in the log plot. We can introduce an effective slope defined as

$$B = \left[ \frac{d\sigma}{d|t|} \right]_0 / \int d|t| \frac{d\sigma}{d|t|} \quad (2.14)$$

which is the inverse of the integral  $\int F(|t|)^2 d|t|$  and varies monotonously from  $B = 7.038 \text{ GeV}^{-2}$  to  $B = 6.839 \text{ GeV}^{-2}$  in the interval  $0 \leq Q^2 < \infty$ .

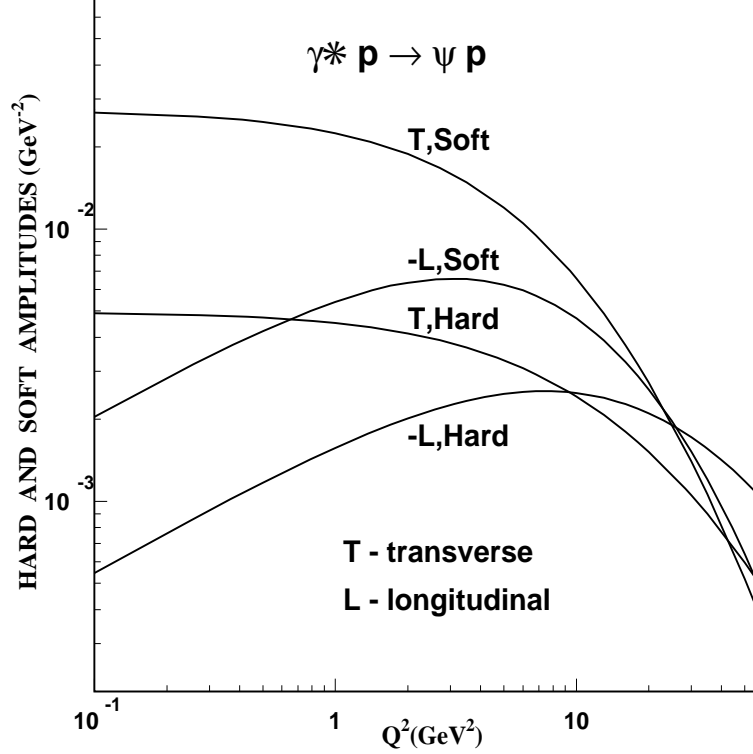


FIG. 1: Hard and soft parts of the reduced amplitudes for transverse and longitudinal polarisations, according to Eqs. (2.11). These functions can be represented by the parametrisations (2.12),(2.13).

In any approach where the wave function of the heavy meson is taken into account [10, 11] nonperturbative quantities like the “meson radius”  $1/\omega$  enter even at the “small” side of the interaction which determines the “hard” scale. It is therefore interesting to study the strictly non-relativistic limit of the meson wave function, where the ratio  $\omega/M_V$  goes to zero and the meson radius drops out in the final expressions for the amplitudes. In this limit, which also implies  $m_f \rightarrow M_V/2$ , all integrals can be performed analytically if we neglect the energy dependence by putting  $\epsilon_s = \epsilon_h = 0$ . We obtain the asymptotic results

$$T_{\gamma^* p \rightarrow Vp}^{\pm 1}(t, Q^2)/(-2is) \approx \frac{C e^{-a|t|}}{1 + b|t|} \frac{\sqrt{3}}{\sqrt{\alpha}} \frac{16}{(Q^2 + M_V^2)^2} M_V^{3/2} \Gamma_{e^+e^-}^{1/2},$$

$$T_{\gamma^* p \rightarrow Vp}^0(t, Q^2) \approx \frac{Q}{M_V} T_{\gamma^* p \rightarrow Vp}^{\pm 1}(t, Q^2). \quad (2.15)$$

In Fig. 2 we show in solid line the full result (with  $\epsilon_h = \epsilon_s = 0$ ) and in dashed line the asymptotic form of (2.15) for forward differential cross section  $\left[ d\sigma/d|t| \right](t=0)$ .

### III. NUMERICAL RESULTS AND COMPARISON WITH EXPERIMENTS

Our numerical calculations presented in the figures below with experimental data are exact evaluations of the model, based on Eqs.(2.1,2.2). However, we stress that Eqs.(2.10,2.11,2.12,2.13) represent very accurately these results.

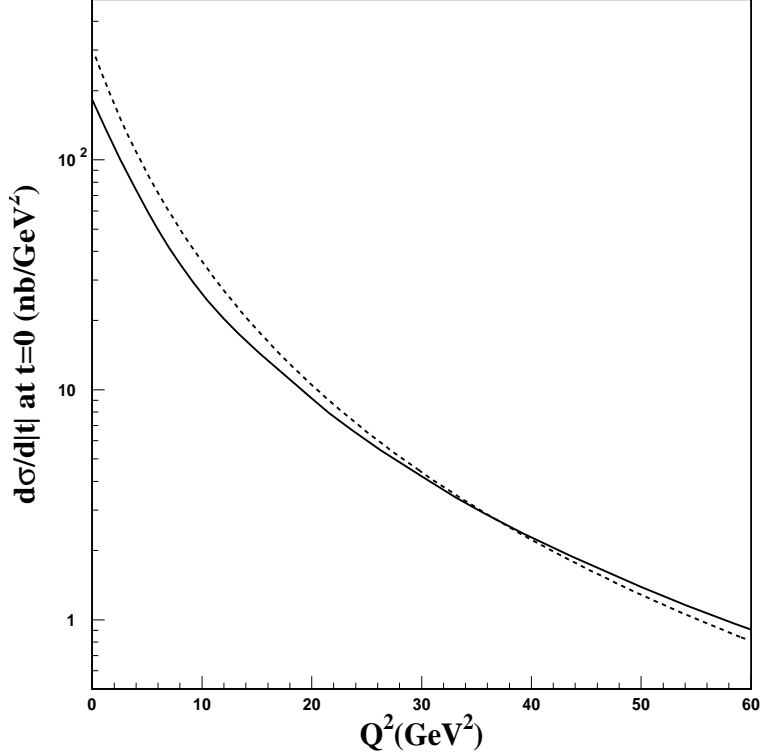


FIG. 2: Influence of the nonperturbative parameters of the  $J/\psi$  meson on the  $Q^2$  dependence of the forward differential cross section. In solid line our calculations without energy dependence ( $\epsilon_h = \epsilon_s = 0$ ) and in dashed line the asymptotic form of Eq. (2.15).

In Fig. 3 we show the integrated  $J/\psi$  production cross section  $\sigma = \sigma_T + \sigma_L$  at  $W = 90$  GeV as a function of  $Q^2$ , together with the HERA data from the H1 and Zeus collaborations [12, 13]. The solid line corresponds to the exact equations (2.1,2.2), while for the dashed line there is a multiplying factor

$$\frac{4\pi/0.57}{11 \log(Q^2 + 7.42)}$$

introduced [14] to take into account the running of the strong coupling in the model which otherwise is purely nonperturbative.

The energy dependence adopted in our model is fully compatible with the existing published data [12, 13, 15, 16] as can be seen in Fig.4. We repeat in this figure our results for photoproduction (empty circles and squares) which have been shown before [1] to agree well with the data.

The energy dependences of the cross section have general forms

$$\sigma_{T,L}(Q^2) = (A_{\text{hard}}^{T,L}(Q^2) W^{2\epsilon_h} + A_{\text{soft}}^{T,L}(Q^2) W^{2\epsilon_s})^2,$$

where  $A_{\text{hard}}^{T,L}(Q^2)$  and  $A_{\text{soft}}^{T,L}(Q^2)$  can be easily calculated from (2.10), (2.12) and (2.13).

Often experimental cross sections are fitted through a single power  $W^{\delta(Q^2)}$ , with  $W = \sqrt{s}$ , which must be used in a limited energy range. For small  $Q^2$  the soft pomeron is important and  $\delta$  is small, but for larger  $Q^2$  the hard pomeron becomes dominant and the exponent

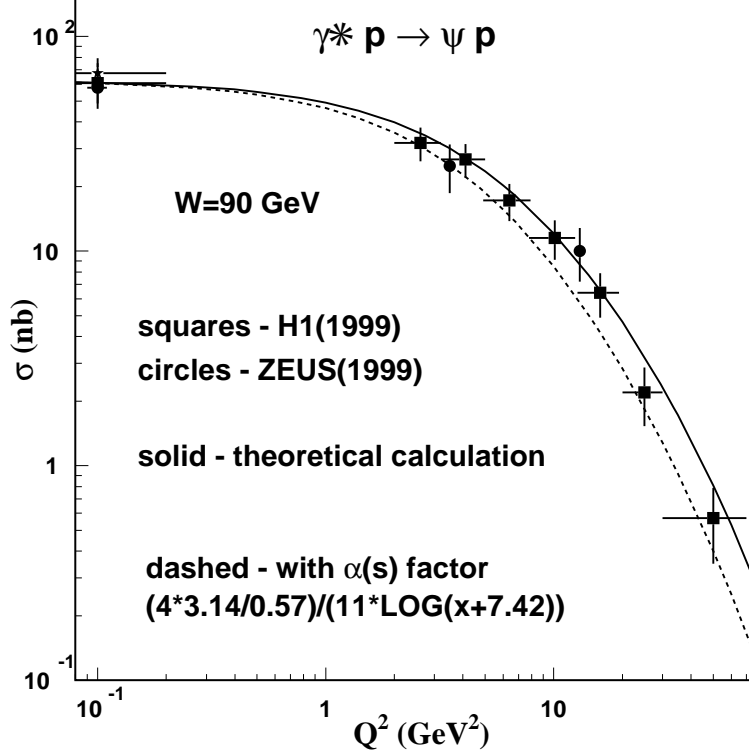


FIG. 3:  $Q^2$  dependence of the integrated elastic cross section  $\sigma = \sigma_T + \sigma_L$  at the energy  $W = 90$  GeV, compared to data from Zeus [12] (circles) and H1 [13] (squares). The full line represents our results as explained in the text. In the dashed line an extra factor is introduced to account for the possible effect of a  $Q^2$  dependence of the running strong coupling constant [14].

$\delta \equiv 4\epsilon_{\text{eff}} \rightarrow 4\epsilon_h = 0.168$  as  $Q^2 \rightarrow \infty$ . A convenient interpolation formula in the range  $20 \leq W \leq 200$  GeV is

$$\epsilon_{\text{eff}}(Q^2) = \epsilon_h - \frac{1}{(3.28 + Q^2/M_V^2)^{1.22}}. \quad (3.1)$$

Our results for the transverse and longitudinal cross sections at  $W = 90$  GeV can be parametrised in the forms

$$\sigma_T(Q^2) = \frac{63}{(1 + Q^2/M_{J/\psi}^2)^{3.17}} \text{ nb} \quad \text{and} \quad \sigma_L(Q^2) = \frac{50 Q^2/M_{J/\psi}^2}{(1 + Q^2/M_{J/\psi}^2)^{3.28}} \text{ nb}. \quad (3.2)$$

The ratio  $R = \sigma_L/\sigma_T$  of longitudinal to transverse cross section is displayed in Fig. 5. The solid line shows our result for  $W = 90$  GeV, which agrees well with the data [12, 13] at the same energy. The dashed line is the asymptotic result  $R_{\text{asympt}} = Q^2/M_{J/\psi}^2$ , from (2.15).

The differential cross section  $d\sigma/d|t|$  and its energy dependence obtained from our model have been shown [1] to describe well the data for  $J/\psi$  photoproduction in a wide energy range. There are no published data of  $d\sigma/d|t|$  for electroproduction to be compared to our calculations, which predict that the shape of the angular distribution is almost independent of  $Q^2$ .

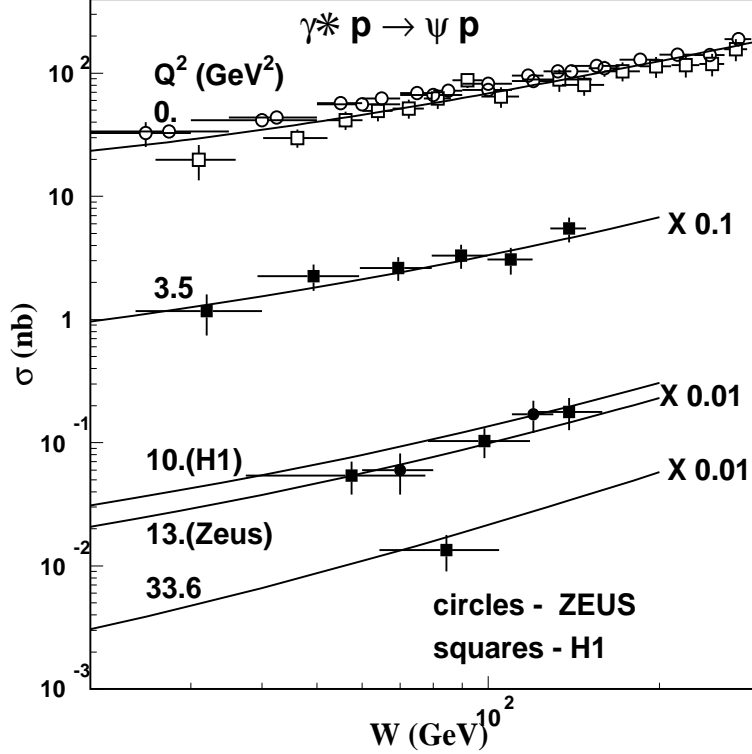


FIG. 4: Energy dependence of the integrated cross section for several values of  $Q^2$  compared to data from Zeus in full [12] and empty [16] circles and from H1 in full [13] and empty [15] squares.

#### IV. CONCLUSIONS

Our nonperturbative model describes the data well. We found that the main features are expressed in the simplified equations (2.10, 2.11, 2.12, 2.13) which represent very well the full results of our model. This is due to the small range of the overlap functions compared to the proton size and to the range of the correlation functions of the QCD vacuum, which determine the interactions in our model. As a consequence of these properties of the amplitudes, in our nonperturbative treatment of the electroproduction of heavy vector mesons (here with particular application to  $J/\psi$  production) some quite general features emerge, which are mainly a consequence of the general approach to high energy scattering [2, 3, 4] and not of the specific stochastic vacuum model [5, 6], which yields the numerical values of the parameters in (2.9).

The main shape of the  $Q^2$  dependence is determined by the overall overlap strength (2.11). Our calculations, which reproduce well the data for  $J/\psi$  production for  $Q^2 \leq 60 \text{ GeV}^2$  deviate considerably from the asymptotic result (2.15) and shows that genuine nonperturbative parameters, like the size of the vector meson ( $1/\omega$ ), have a considerable influence even on the “hard part” of the interaction.

Fig. 4 shows that the  $W$ -dependence based on the two-pomeron model [9] is appropriate to describe the existing data.

In the ratio  $R = \sigma_L/\sigma_T$  the characteristic numbers coming from the stochastic vacuum model nearly cancel out, as can be seen in (2.8), and the ratio depends solely on the overlap strengths defined in (2.11). Due to the energy dependence induced by the overlap function,



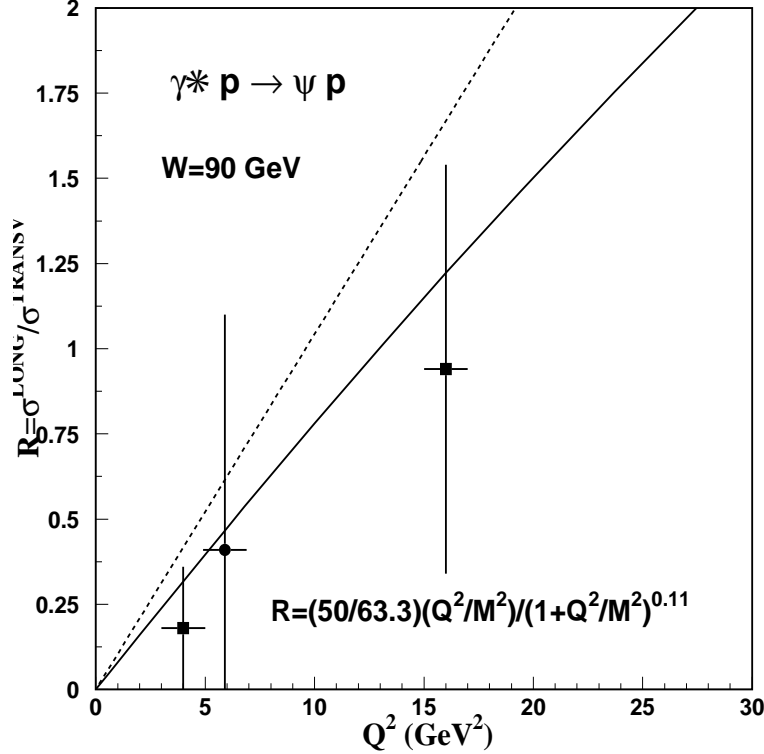


FIG. 5: Ratio between longitudinal and transverse cross sections at  $W = 90$  GeV as a function of  $Q^2$  compared to the data from Zeus [12] (circle) and H1 [13] (squares) collaborations. The solid line is our theoretical result, for which we give a parametrization. The dashed line represents the asymptotic calculation (size zero for the vector meson).

see (2.10,2.11), the ratio will also exhibit a characteristic energy dependence. At  $W = 90$  GeV the ratio agrees reasonably well with the data shown in Fig. 5. It is important to check this result against future data at other energies and for a wider range of  $Q^2$ .

The predicted  $t$  dependence is nearly universal, namely independent of  $Q^2$  and  $W$ , with only small corrections due to the term  $e^{-\eta R_1^2 |t|}$  in (2.8) and slight dependence on  $W$  due to the different energy factors controlling the couplings of small and large dipoles.

### Acknowledgments

The authors wish to thank DAAD(Germany), CNPq(Brazil), CAPES(Brazil) and FAPERJ(Brazil) for support of the scientific collaboration program between Heidelberg, Frankfurt and Rio de Janeiro groups working on hadronic physics.

- 
- [1] H.G.Dosch and E.Ferreira, Eur. Phys. J. C **29** (2003) 45
  - [2] H.G. Dosch, E. Ferreira and A. Kramer, Phys. Rev. D **50** (1994) 1992
  - [3] H. G. Dosch, T. Gousset, G. Kulzinger and H. J. Pirner, Phys. Rev. D **55** (1997) 2602
  - [4] O. Nachtmann, Annals Phys. **209** (1991) 436.

- [5] H. G. Dosch, Phys. Lett. B **190** (1987) 177.
- [6] H. G. Dosch and Y. A. Simonov, Phys. Lett. B **205** (1988) 339.
- [7] A. I. Shoshi, F. D. Steffen, H. G. Dosch and H. J. Pirner, Phys. Rev. **D66**: 094019 (2002)
- [8] M. Bauer, B. Stech and M. Wirbel, Z. Phys. C **34** (1987) 103.
- [9] A. Donnachie and P. V. Landshoff, Phys. Lett. B **437** (1998) 408
- [10] J. Nemchik, N.N. Nikolaev, E. Predazzi and B.G. Zakharov, Z. Phys. C **75**, 71 (1997)
- [11] J. Hüfner, Yu.P. Ivanov, B.Z. Kopeliovich and A.V. Tarasov, Phys. Rev. D **62**, 094022 (2000)
- [12] J. Breitweg et al., Zeus Coll., Eur. Phys. J. C **6** (1999) 603
- [13] C. Adloff et al., H1 Coll. Eur. Phys. J. C **10** (1999) 373
- [14] A. Donnachie and H. G. Dosch, Phys. Rev. D **65** (2002) 014019
- [15] C. Adloff et al., H1 Coll. Phys. Lett. B **483** (2000) 23
- [16] S. Chekanov et al., Zeus Coll., Eur. Phys. J. C **24** (2002) 345